Chinese Chemical Letters 34 (2023) 107580

Contents lists available at ScienceDirect

Chinese Chemical Letters

journal homepage: www.elsevier.com/locate/cclet

Room-temperature synthesis of layered open framework cathode for sodium-ion batteries

Ruding Zhang [a,b], Huixin Chen [a,b], Hongjun Yue [a,b,*]

[a] CAS Key Laboratory of Design and Assembly of Functional Nanostructures, and Fujian Provincial Key Laboratory of Nanomaterials, Fujian Institute of Research on the Structure of Matter, Chinese Academy of Sciences, Fuzhou 350002, China
[b] Xiamen Key Laboratory of Rare Earth Photoelectric Functional Materials, Xiamen Institute of Rare Earth Materials, Haixi Institutes, Chinese Academy of Sciences, Xiamen 361021, China

ARTICLE INFO

Article history:
Received 5 May 2022
Revised 21 May 2022
Accepted 1 June 2022
Available online 3 June 2022

Keywords:
Room temperature solution synthesis
Open framework structure
Cathode materials
Sodium-ion batteries
Full cell

ABSTRACT

The synthesis of active electrode materials at room temperature is one of the effective strategies to reduce the fabrication cost of sodium ion batteries (SIBs). Herein, a layered material $(Na_2[(VO)_2(HPO4)_2C_2O_4]\cdot 2H_2O$, abbreviated as NVPC followingly) with open-framework structures has been successfully prepared at room temperature under ambient conditions and is evaluated as a cathode for SIBs. It is revealed that NVPC cathode can deliver a maximum reversible capacity of *ca.* 70 mAh/g at 10 mA/g, and exhibit superior rate capability and cycling performance: at 50 mA/g, maximum reversible capacity *ca.* 50 mAh/g with capacity retention of 88.4% over 250 cycles corresponds to only 0.046% capacity decay per cycle; at 100 mA/g, a maximum reversible capacity of 35 mAh/g with capacity retention of 60.9% over 500 cycles. This study demonstrates a practical example of a low-cost synthesis of the cathode materials for SIBs. At the same time, the systematic electrochemical research results also show promising prospects for long lifespan low-cost SIBs.

As an alternative and supplementary technology to lithium-ion batteries (LIBs), the potential low-cost sodium-ion batteries (SIBs) have been intensively investigated and are expected to satisfy the urgent demand for large-scale stationary electricity energy storage systems for the future applications since sodium could release the anxiety of Li-resource scarcity owing to the abundant natural reserves and geographically widespread distribution of sodium resources [1–5]. Currently, some encouraging progress has been appropriately achieved on varieties of low-cost and high-performance electrode materials for SIBs, especially cathode materials [6–10]. However, due to the relatively large radius of Na-ion (1.02 Å *vs.* 0.76 Å for Li-ion), these existing materials are often faced with the following problems such as short lifespan, inferior cyclability, and poor structural stability [11,12], and which seriously hinders the further development of SIBs. Therefore, it is still a lack of feasible cathode materials that can accommodate reversible insertion/extraction of the large-sized Na-ions.

Apart from the need to explore new electrode materials, the cost of electrode materials, mainly composed of raw materials cost and manufacturing costs, is also one of the critical factors that must be considered in promoting the industrialized application of SIBs [13]. It is widely accepted that the cost of materials production accounts for a large proportion of the total energy cost of an electrochemical device [14,15]. Currently, the relatively common and popular method used to prepare cathode materials often involves the solid phase calcination process, which is finished at a very high temperature [16,17]. Undoubtedly, this high energy consumption process increases the cost of the whole fabrication process and the total cost of an electrochemical system invisibly. Therefore, it is significant to develop low energy consumption ways for the production of active materials, of which the straightforward room temperature (RT) solution routines for the preparation of cathode materials could be a potential direction.

Based on these two aspects of consideration and analysis, here in this study, we propose a simple solution method for synthesizing a layered cathode material $(Na_2[(VO)_2(HPO_4)_2C_2O_4]\cdot 2H_2O$, abbreviated as NVPC followingly) by stirring the mixture of reactant precursors at RT under ambient conditions. It is demonstrated that NVPC crystalizes in a layered structure with open frameworks. Systematic electrochemical test results uncovered that NVPC cathode could deliver a discharge capacity of ~70 mAh/g at 10 mA/g cur-

* Corresponding author at: CAS Key Laboratory of Design and Assembly of Functional Nanostructures, and Fujian Provincial Key Laboratory of Nanomaterials, Fujian Institute of Research on the Structure of Matter, Chinese Academy of Sciences, Fuzhou 350002, China.
E-mail address: hjyue@fjirsm.ac.cn (H. Yue).

https://doi.org/10.1016/j.cclet.2022.06.003
1001-8417/

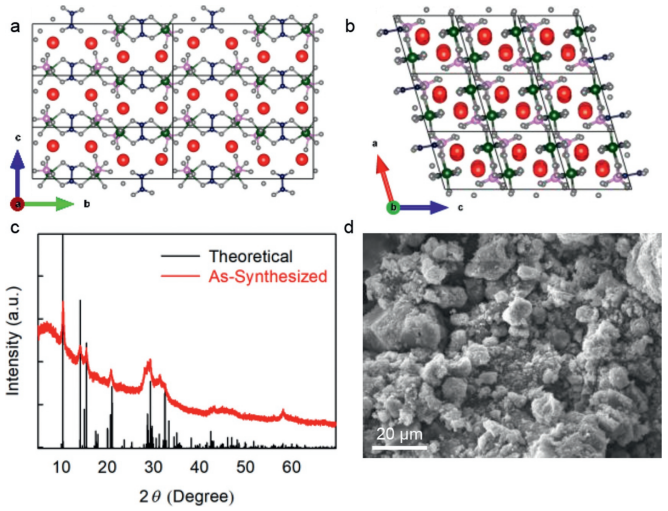

Fig. 1. (a, b) Crystal structure representation of NVPC displayed along a-axis and b-axis, respectively; V, P, Na, O and C atoms are shown as bluish green, light purple, red, gray, and light blue balls, respectively; H_2O in the interlayers is not shown for clarity. (c) XRD partten of the as-obtained NVPC sample. (d) SEM image of NVPC particles.

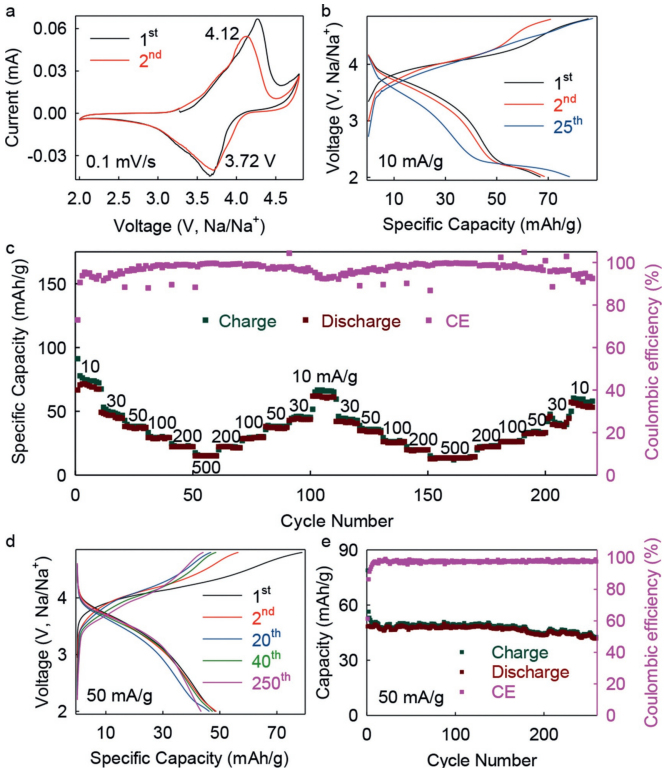

Fig. 2. (a) CV profiles of the NVPC electrode at a scan rate of 0.1 mV/s. (b) The selected cycling voltage profiles of the NVPC electrode at a current density of 10 mA/g. (c) Rate capability of NVPC electrode. (d, e) Long-term cyclability and corresponding voltage profiles at 50 mA/g.

rent density and even maintain ~35 mAh/g at 100 mA/g current rate. Morever, a high capacity retention of 88.4% corresponding to only 0.046% capacity decay per cycle after 250 cycles at 50 mA/g and 60.9% after 500 cycles at 100 mA/g have also been obtained. The simple and low energy consumption synthesis strategy coupled with outstanding electrochemical performance suggests the possible commercial application of NVPC cathode in SIBs.

The crystal structure views of NVPC (Figs. 1a and b, Fig. S1 in Supporting infomation) show that NVPC crystallizes into a typical layered structure, in which sodium ions reside between the two-dimensional interlayer space. Specifically, as shown in Fig. S1, the one-dimensional $VOHPO_4$ chains composed of VO_6 moieties and HPO_4 units are interlinked by the oxalate ligands to form two-dimensional infinite anionic sheets of $[(VOHPO_4)_2(C_2O_4)]_n^{2n-}$. These two-dimensional anionic layers are further bonded to the counter ions-Na-ions. This unique sandwich-like open framework structure provides the opportunity for reversible Na^+ extraction and insertion. XRD patterns were collected to investigate the structure and phase information of the obtained NVPC active materials. As shown in Fig. 1c, the XRD pattern indicates the highly pure and well crystalline of NVPC, indexed to the monoclinic phase with a space group of P 2_1. The well-defined, strong diffraction peaks at $2\theta = 10.3°$, 14.06°, 15.42° and 20.98° are ascribed to the reflection of (020), (001), (110) and (031) crystal planes of NVPC, respectively. NVPC presents an irregular particle morphology as revealed by the SEM image in Fig. 1d.

To elucidate the electrochemical sodium-ions extraction/ insertion behavior of NVPC, we take the half cell configuration with Na foil as the counter & reference electrode and NVPC cathode as the working electrode to conduct the cyclic voltammograms (CVs) and galvanostatic sodiation/de-sodiation (GSD) measurements. A typical cyclic voltammetry (CV) measurement for the initial two cycles at 0.1 mV/s was carried out to investigate the redox behavior of the NVPC electrode (Fig. 2a). The prominent oxidic peak around 4.12 V followed by a clear cathodic peak at 3.72 V in the first cycle represents a reversible Na^+- deintercalation/intercalation occurring in NVPC. The almost overlapped CV curve with the first cycle indicates highly reversible Na^+ (de)sodiation chemistry during the second cycle. GSD test with a current density of 10 mA/g in the voltage window of 2.0–4.8 V *versus* Na at RT was conducted to probe the maximum sodium-storage capacity of the NVPC cathode. At 10 mA/g, NVPC gives a maximum reversible discharge capacity of *ca.* 70 mAh/g, which corresponds to the insertion of 0.65 Na^+ per formula unit and a high average discharge voltage of ~3.5 V (Fig. 2b and Fig. S2 in Supporting information). The value of Coulombic efficiency (CE) in the initial GSD cycle is just 78%, which can be attributed to the contribution of irreversible decomposition of electrolytes. Also, we notice a slight increase in the specific capacity during the initial cycles, representing a successive activation process caused by repeated Na^+-deintercalation/intercalation cycles, a normal phenomenon often appears during battery cycling [11,18–20].

Figs. 2c–e, Figs. S3 and S4 (Supporting information) display the rate and long-term cycle performance of the NVPC electrode at the current density of 10, 30, 50, 100, 200 and 500 mA/g, respectively. NVPC cathode exhibited an outstanding rate capability, reflecting that reversible capacities of 71, 40, 30 and 16 mAh/g at current rates of 10, 50, 100 and 500 mA/g could achieve, respectively (Fig. 2c). Furthermore, the corresponding capacity can return to the initial state when the current density is set back to 10 mA/g. Of equal importance, the reversible capacity returns to ~70 mAh/g after two repeated rate cycling, confirming the structural stability of this cathode. Corresponding GSD voltage profiles of different current rates presenting similar curve shapes again confirm the superior rate performance and suggest the structural stability of the NVPC electrode (Fig. S3). According to the long-term cyclability depicted in Figs. 2d and e, Fig. S4, the NVPC-based battery realized capacity retention of 88.4% over 250 cycles with an average CE over 98% (from the second cycle to the afterward cycles) at a moderate current rate of 50 mA/g. Under a high current density of 100 mA/g, maximum reversible capacity *ca.* 35 mAh/g with capacity retention of 60.9% over 500 cycles and an average CE over 99% was also achieved (from the second cycle to the afterward cycles). Such excellent rate capability and considerable long-term cyclability sug-

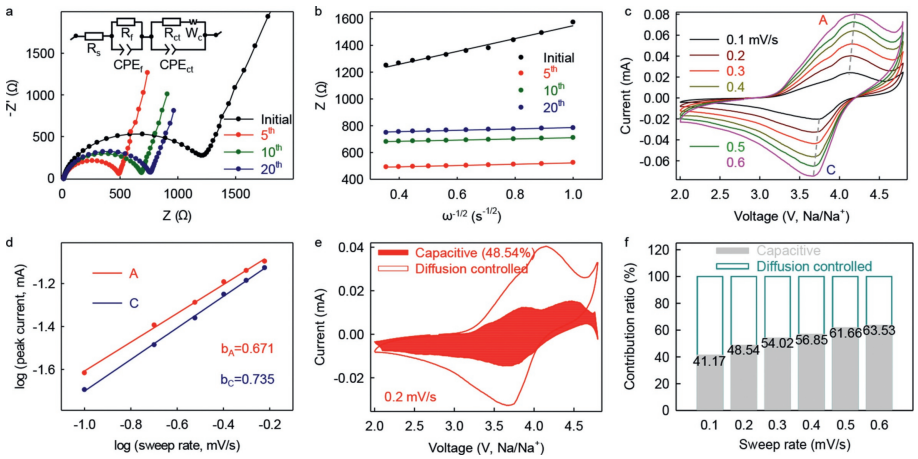

Fig. 3. (a) Nyquist plots of the NVPC electrodes after different cycles (inset: selected equivalent circuit). (b) The linear fits of the real impedance *versus* square root of frequency in the low-frequency region. (c) CV profiles at different scan rates. (d) Log(peak current) *versus* log(scan rate) and corresponding *b*-values. (e) CV curve with the pseudocapacitive and diffusion contribution at 0.2 mV/s. (f) Bar chart of the percentages of pseudocapacitive contributions at different sweep rates.

gest the relatively high structural stability of NVPC and relatively rapid Na^+ diffusion within it.

To gain the kinetic insights into the Na-ions storage chemistry in this layered compound electrode, electrochemical impedance spectroscopy (EIS), rate-scan CV, and galvanostatic intermittent titration technique (GITT) electrochemical tests were carried out. The EIS test results shown in Fig. 3a show that the charge transfer resistance (R_{ct}) gradually decreases and roughly stabilizes in a certain state during the first 20 GSD cycles, reflected by the variation trend of semicircle radius in Nyquist plots. This successive activation process is following the observation of GSD test. The relatively small R_{ct} also promises relatively fast charge transfer in the NVPC cathode, which would have been conducive to the superior rate properties. Through fitting the slope line part in Nyquist plots at low-frequency range, we derived the Na-ion diffusion coefficient (D_{Na}) is 10^{-14} cm^2/s (Fig. 3b) in the first cycle due to incomplete activation, and then the D_{Na} values are maintained to be in the order of 10^{-12} cm^2/s (Fig. 3b) after activation process according to the reported equation [21]. In addition, D_{Na} in the NVPC electrode can also be assessed by GITT and rate-scan CV technique. As depicted in Figs. S5 and S6 (Supporting information), the value of D_{Na} are calculated to be in the order of 10^{-12} to 10^{-11} cm^2/s by the Weppner-Huggins equation [22] and in the order of 10^{-12} cm^2/s by the Randles-Sevcik equation [23], respectively. In addition, from GITT results shown in Fig. S5, we observed that as the intercalation reaction happens, the diffusion coefficients of Na^+ change with the electrochemical reaction going on and this phenomenon is line with the observation of the reported results [24–27]. We suspect that the variation of Na^+ number in NVPC host, the variation of the interaction between Na^+ and NVPC frameworks, and the variation of effective contact area of active materials and electrolyte with formation of CEI are possibly responsible for the changing diffusivity.

In addition, to further analyze the redox pseudocapacitance-like contribution from the perspective of the electrochemical kinetics, the CVs under different scan rates from 0.1 mV/s to 0.6 mV/s were carried out. It is well recognized that the relationship between the peak current (i) and the scan rate (v) can be expressed by the equation of $i = av^b$, where a and b are adjustable parameters [28]. The b-value corresponding to redox peaks A and C are determined to be 0.671 and 0.735 from the slope of the log(i) *versus* log(v) plot, respectively, (Figs. 3c–f), suggesting an ionic diffusion-dominant kinetic process for NVPC cathode electrochemical behavior due to that both values of b are relatively closer to 0.5. Furtherly, the contribution ratio of capacitive (k_1) and diffusion (k_2)

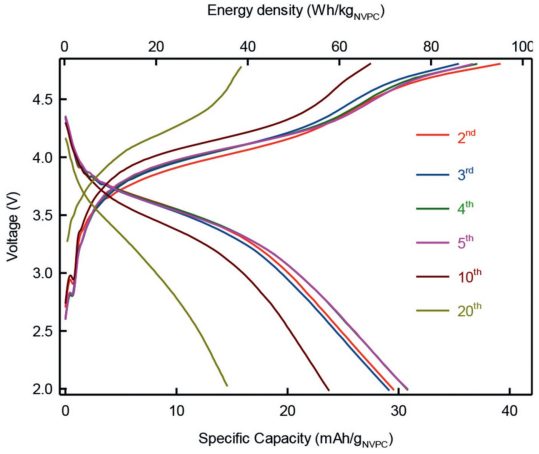

Fig. 4. Electrochemical curves of the full battery cycled at 10 mA/g in 1 mol/L $NaClO_4$ electrolyte tested at 2.0–4.8 V.

under different scan rates can be quantified according to the equations of $i = k_1v + k_2v^{1/2}$ and $i/v^{1/2} = k_1v^{1/2} + k_2$, where k_1v means pseudocapacitive effect and $k_2v^{1/2}$ represents the contribution of ionic diffusion-controlled, respectively [29]. The detailed capacitive fractions were deduced to 41.17% be and 48.54% at low scan rates of 0.1 mV/s and 0.2 mV/s, respectively. Also, the percentage of the capacitive contribution increases with the scanning rate increases, and the capacitive contribution reaches 63.53% at 0.6 mV/s (Fig. S7 in Supporting information).

To verify the application prospect, full SIBs are assembled in the configuration of NVPC//$NaClO_4$-based electrolyte//carbon P. Carbon P was purchased without any further treatment for anode use. As depicted in Fig. 4 and Fig. S9 (Supporting information), the full SIB delivers a moderate discharge capacity of ~30 mAh/g based on the mass of NVPC cathodes. The charge and discharge curves show that the full battery outputs an average discharge voltage of ~3.3 V (Fig. 4 and Fig. S8 in Supporting information). The energy density of the full SIB is high, up to ~100 Wh/kg_{NVPC}. Such superior electrochemical performance suggests promising applications of SIBs in large-scale electric energy storage.

In conclusion, a cathode material (NVPC) with open frameworks was successfully prepared through a mild room temperature solution method with a low energy consumption route and proposed a electrode for SIBs. Systematic electrochemical studies revealed that NVPC cathode could deliver a considerable reversible capac-

ity of 70 mAh/g and exhibit superior rate capability and cycling performance. Specifically, reversible capacity 50 mAh/g with capacity retention of 88.4% over 250 cycles corresponding to only 0.046% capacity decay per cycle and reversible capacity 35 mAh/g with capacity retention of 60.9% over 500 cycles can be both realized in this electrode at a moderate current rate of 50 mA/g and a high current density of 100 mA/g, respectively. Overall, our results provide new insight into SIBs electrode materials development for low-cost and large-scale energy-storage applications.

Declaration of competing interest

The authors declare that they have no known competing financial interests or personal relationships that could have appeared to influence the work reported in this paper.

Acknowledgment

This work was financially supported by the National Natural Science Foundation of China (No. 21805278).

Supplementary materials

Supplementary material associated with this article can be found, in the online version, at doi:10.1016/j.cclet.2022.06.003.

References

[1] N. Yabuuchi, K. Kubota, M. Dahbi, S. Komaba, Chem. Rev. 114 (2014) 11636–11682.
[2] D. Kundu, E. Talaie, V. Duffort, L.F. Nazar, Angew. Chem. Int. Ed. 54 (2015) 3431–3448.
[3] R.C. Massé, E. Uchaker, G. Cao, Sci. Chin. Mater. 58 (2015) 715–766.
[4] B. Liu, D.N. Lei, J. Wang, et al., Nano Res. 13 (2020) 2136–2142.
[5] S.Y. Li, W. He, B. Liu, et al., Energy Storage Mater. 25 (2020) 636–643.
[6] J. Kim, H. Kim, K. Kang, Adv. Energy Mater. 8 (2018) 1702646.
[7] B. Senthilkumar, C. Murugesan, L. Sharma, S. Lochab, P. Barpanda, Small Methods 3 (2018) 1800253.
[8] Y. Sun, S. Guo, H. Zhou, Adv. Energy Mater. 9 (2018) 1800212.
[9] J. Feng, S. Luo, K. Cai, et al., Chin. Chem. Lett. 33 (2022) 2316–2326.
[10] A.S. Hameed, M. Ohara, K. Kubota, S. Komaba, J. Mater. Chem. A 9 (2021) 5045–5052.
[11] N.T. Aristote, K. Zou, A. Di, et al., Chin. Chem. Lett. 33 (2022) 730–742.
[12] N.O. Vitoriano, N.E. Drewett, E. Gonzalo, T. Rojo, Energy Environ. Sci. 10 (2017) 1051–1074.
[13] C. Vaalma, D. Buchholz, M. Weil, S. Passerini, Nat. Rev. Mater. 3 (2018) 18013.
[14] D. Larcher, J.M. Tarascon, Nat. Chem. 7 (2015) 19–29.
[15] R. Schmuch, R. Wagner, G. Hope, T. Placke, M. Winter, Nat. Energy 3 (2018) 267–278.
[16] C. Zhao, F. Ding, Y. Lu, L. Chen, Y.S. Hu, Angew. Chem. Int. Ed. 59 (2020) 264–269.
[17] C. Yang, S. Xin, L. Mai, Y. You, Adv. Energy Mater. 11 (2020) 2000974.
[18] Y. Dai, Q. Chen, C. Hu, et al., Chin. Chem. Lett. 33 (2022) 1435–1438.
[19] R. Zhang, J. Bao, Y. Wang, C.F. Sun, Chem. Sci. 9 (2018) 6193–6198.
[20] R.D. Zhang, J.J. Huang, W.Z. Deng, et al., Angew. Chem. Int. Ed. 58 (2019) 16474–16479.
[21] C. Ho, I. Raistrick, R. Huggins, J. Electrochem. Soc. 127 (1980) 343.
[22] W. Weppner, R.A. Huggins, J. Electrochem. Soc. 12 (1977) 1569–1578.
[23] D.Y.W. Yu, C. Fietzek, W. Weydanz, et al., J. Electrochem. Soc. 154 (2007) A253–A257.
[24] X. Han, W.J. Zhou, M.F. Chen, et al., Nano Res. 15 (2022) 6156–6167.
[25] H.Y. Wang, H.X. Chen, C. Chen, et al., Chin. Chem. Lett. 34 (2023) 107465.
[26] M.T. Cai, H.H. Zhang, Y.G. Zhang, et al., Sci. Bull. 67 (2022) 933–945.
[27] Q. Zhang, Y.P. Zeng, C.S. Ling, et al., Small 18 (2022) 2107514.
[28] H.S. Kim, J.B. Cook, H. Lin, et al., Nat. Mater. 16 (2017) 454.
[29] J. Wang, J. Polleux, J. Lim, B. Dunn, J. Phys. Chem. C 111 (2007) 14925.